A Raman spectroscopy study of the oxidation processes in synthetic chromite $FeCr_2O_4$

Vanni Lughi [1], Davide Lenaz [2, 3], Alois Bonifacio [1], Francesco Princivalle [3], Valter Sergo [1] and Filippo Parisi [2, 3,*]

Department of Engineering and Architecture, University of Trieste, Trieste, I-34128 Italy;
Department of Mathematics and Geosciences, University of Trieste, Trieste, I-34128 Italy;
Department of Physics and Chemistry, University of Palermo, Palermo, I-90128 Italy;

*Correspondence: filippo.parisi@unipa.it;

ABSTRACT. A crystal of synthetic chromite $FeCr_2O_4$ has been annealed in air at 700°C for 50 days at room pressure in order to study physical-chemical changes. After the annealing treatment, Scanning Electron Microscopy (SEM) images of the polished surface of the sample showed areas of different composition. Detailed Raman mapping revealed that the annealed chromite undergoes an oxidation process, proceeding inwards from the outer surface and leading to the transformation of chromite to magnetite, and ultimately to hematite. The oxidation process also leads to the formation of trellis-like lines, arguably via stress-related mechanisms associated with the phase transformation and consequent volume changes. The present study confirms the possibility of non-stoichiometry or structural defects causing slight structural asymmetries and the formation of new modes, resulting in a valuable support in characterizing both natural and artificial material. The potential of Raman spectroscopy in the identification and spatial resolution of mineralogical phases, is also highlighted.

Keywords: spinel, chromite, magnetite, hematite, oxidation, Raman mapping

1. Introduction

Chromite is an oxide mineral belonging to the spinel group with ideal formula $FeCr_2O_4$. Its interesting properties are not limited to the chromium content used for industrial applications but are still in the spotlight of researchers for many reasons[1–3] including its high thermal stability[4,5]. The chromite end-member $Fe^{2+}Cr_2O_4$ is a typical example of a normal spinel where the divalent cation fills only the tetrahedral site (T) and the trivalent cations fill the octahedral one (M). This fact is due to the large excess octahedral crystal field stabilization energy of Cr^{3+} ensuring its preference for the octahedral site[6,7].

Natural spinels can only approximate the ideal $FeCr_2O_4$, in fact, other cations may enter into the crystal structure, so that $(Mg, Fe^{2+})(Al, Cr^{3+})_2O_4$ better describes natural Cr-bearing spinels, with extraterrestrial chromites better approximating the end-members[8,9]. Another cation that could be accommodated in different amounts into the crystal structure is Fe^{3+}. Several authors studied the

effects of Fe^{3+} into the crystal lattice of Cr-bearing spinel and found that it can be present both in tetrahedral (T) and octahedral (M) sites and that in large amounts it creates a magnetite/magnesioferrite component leading to an inverse spinel[10–16]. The main possible causes of the presence of Fe^{3+} within the spinel structure are a higher oxygen fugacity of the original melt from which the spinels form, an oxidation process taking place after spinel formation or the unavailability of other trivalent cation in the melt[10,17–22].

From a chemical point of view, in natural spinels one of the effects of oxidation is the formation of a rim enriched in Fe^{3+} usually called "ferritchromite", but the way it develops and the enrichment or impoverishment of different cations and their exchange with the environment are still a matter of debate due to exchange with other mineral phases present in the surrounding environment. Ferritchromite rims formed at the edges of Cr-spinel crystals have been extensively documented at temperature higher than about 500°C. Velicogna and Lenaz (2017) [23] studied some natural crystals of Cr-bearing spinels containing variable Cr and total iron content (0.1-1.5 and 0.2 – 1.0 atoms per formula unit, respectively) by X-ray single crystal diffraction at ambient conditions and after heating at 600°C for 7 and 28 days in order to verify if they suffered oxidation. The results suggested that air oxidation was absent in the studied natural spinels annealed at 600°C. Some corrosion studies on stainless steel have been performed in order to see what is the effect of oxidation by O_2 and O_2+H_2O on Fe, Cr alloys[24,25].

In order to shed light in this field, two pure $Fe^{2+}Cr_2O_4$ spinelides, where the presence of Fe^{3+} was excluded by Electron microprobe analysis [26], had been annealed in air at 600°C and 700°C for different times (about 120 and 50 total days respectively). Backscattered SEM images of the surface polished chromites after annealing, showed no changes in the crystal heated at 600°C after 120 days, while the sample heated at 700°C showed interesting modifications i.e. the formation of trellis-like lines and a progressive greyscale darkening from the inner core to the rim. The aim of this work is to study the physico-chemical effects of the oxidation on the single crystal of chromite heated at 700°C by Raman spectroscopy. More specifically, we use Raman mapping and statistical spectral analysis to provide detailed compositional information with high lateral resolution and with minimal sample preparation.

2 Materials and Methods

Pure $FeCr_2O_4$ (chromite) spinelides crystals were synthesized by flux-grown method at the Department of Mineralogy of the Museum of Natural History of Stockholm (Sweden) following the procedure described in literature[26,27].

Two different samples of the synthetic crystals were annealed in air at atmospheric pressure at 700 °C for 50 days and 600°C for 120 days, respectively. Successively annealed crystals were thinned, polished, and then analyzed by Electron MicroProbe Analysis (EMPA) coupled to a SEM operated in the backscattering mode.

The Raman spectra were collected by an inVia Raman Microprobe (Renishaw), using a HeNe excitation laser at 632.8 nm, a 50x objective with 0.75 NA, and a 1800 lines/mm grating. The power at the sample surface was 15 mW. An array of 18900 spectral points was collected by an automated mapping system over an area of about 180 x 25 μm on the polished surface of the annealed chromite, as depicted in Figure 2, with a collection time of 1 second per spectrum. In Raman mapping, such an array is referred to as "hyperspectral data set". This data set has then been subjected to a Hierarchical Cluster Analysis (HCA)[28,29] where spectra are grouped according to their similarity.

3. Results

In Figure 1 Electron backscattering images allows to recognize areas with different shades of gray. The chromite annealed at 600°C for 120 days (Fig.1a) has a uniform color proving to be almost unaffected by the treatment except for the big black spots that are visible in Figure 1a. These spots are due to preexistent holes in the crystal structure whose presence becomes evident after the polishing procedure. The crystal annealed at 700°C (Fig. 1b) seems to be more interesting and for that, it was chosen for the Raman mapping. More in details, the inner core is almost clear, turning to a darker shade in proximity of the rim. Within the core and parallel to the 111 lattice planes some trellis lines are recognized.

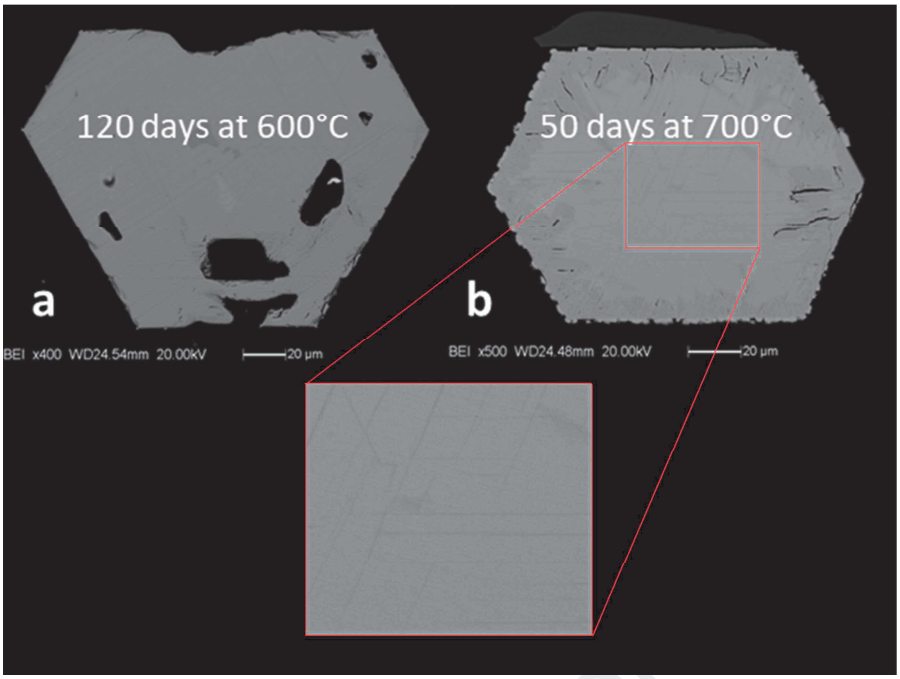

Figure 1. Backscattered SEM images of two surface polished chromites after annealing at 600°C and 700°C for 120 and 50 days, respectively. In the inset, enlargement of the appeared trellis lines parallel to the 111 lattice planes.

The result of the Hierarchical Cluster Analysis (HCA) is shown in Figure 2 and we report the subdivision in 12 clusters (the clustering procedure is arbitrary and it is guided by the similarity of the mean spectrum of the cluster with the spectrum of a known compound), where each color corresponds to a different cluster.

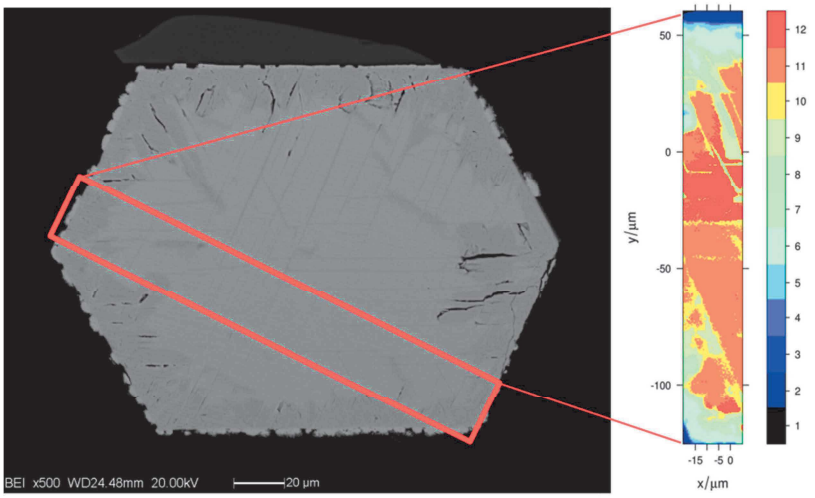

Figure 2. (Left) Backscattered SEM image of the chromite's polished surface after annealing at 700°C, showing the area where the array of spectra was collected from. (Right) Map representing the hierarchical cluster analysis of the array of spectra. Each color in the scale represents the mean of one of the twelve clusters of spectra and allows to determine the location of the different compounds that each cluster represents, as reported in Figure 2

The mean (centroid) of all spectra belonging to each cluster are represented in Figue 3 by using the same color code as in the map of Figure 2; each mean spectrum will be treated as representative of all spectra belonging to the corresponding cluster. Spectra in the orange and red zones (cluster 11 and 12) are essentially identical and will be treated as such in the following.

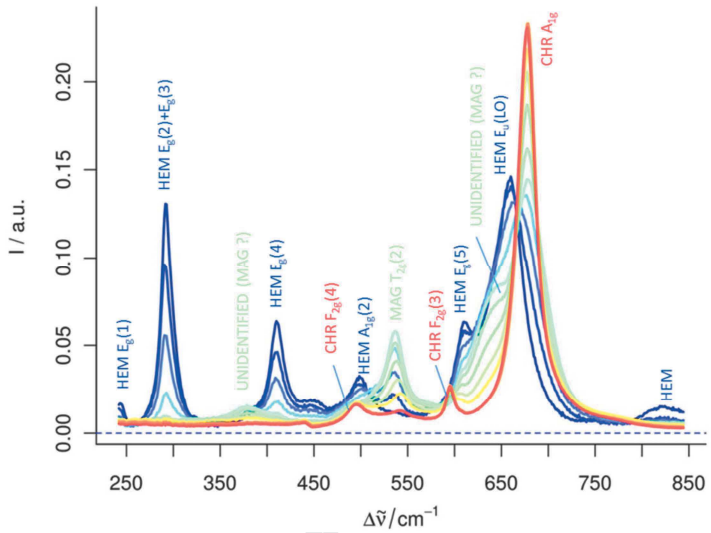

Figure 3. Mean spectra (centroids) of the clusters obtained from the hierarchical cluster analysis. The spectrum representing cluster 1 – corresponding to the resin surrounding the sample – is not included. The color code corresponds to that used for the map in Figure 2. The peaks are labeled according to the known vibrational mode assignments. The abbreviations used are the following: HEM: hematite; MAG: magnetite; CHR: chromite)

The black-colored areas on the map (corresponding to the cluster marked as "1" in the color legend) correspond to the resin surrounding the sample, used for embedding and polishing it, and will be neglected in the following analysis. As shown in Figure 3 most of the peaks observed in the spectra have been identified, according to the available literature[30–35], as belonging to chromite, magnetite, and hematite phases; a more detailed discussion about the vibrational mode assignments is given in the following section. No peaks associated with the vibrational modes of maghemite were observed. A close look at the spectral series reveals the following qualitative observations: spectra corresponding to clusters 11 and 12 (orange and red) can be associated with essentially pure chromite. Spectra representing cluster 7 through 10 (green to yellow) correspond to a mixture of chromite and magnetite; spectra representing cluster 3 through 6 (blue shades) correspond to a mixture of chromite, magnetite, and hematite; finally, the spectrum representing cluster 2 corresponds almost exclusively to a hematite phase.

For a quantitative analysis, the spectra were deconvoluted by using a fitting procedure based on pseudo-Voigt line shapes function, representing a convolution of a Lorentzian and a Gaussian line

shape[36]. This method revealed as the most effective for accurately determine line widths and peak positions in Raman spectra [37–39]. Perusal of the spectra reveals a monotonic increase of the volume fraction of chromite from area 2 to 11-12, a monotonic decrease of hematite from area 2 to 7 (whereas it is absent from area 8 to 11-12), an increase of magnetite from area 2 to 7, followed by a decrease from area 8 to 11-12. The volume fractions are represented in Figure 4 and are calculated based on the approximate assumption that the Raman signal, i.e. the sum of the integrated intensities of all peaks associated to a specific phase, is simply proportional to the volume fraction of that phase. For the chromite, the sole peak at 672 has been used for quantifying the phase, since the other two were too small and covered by other peaks in the mixed spectra.

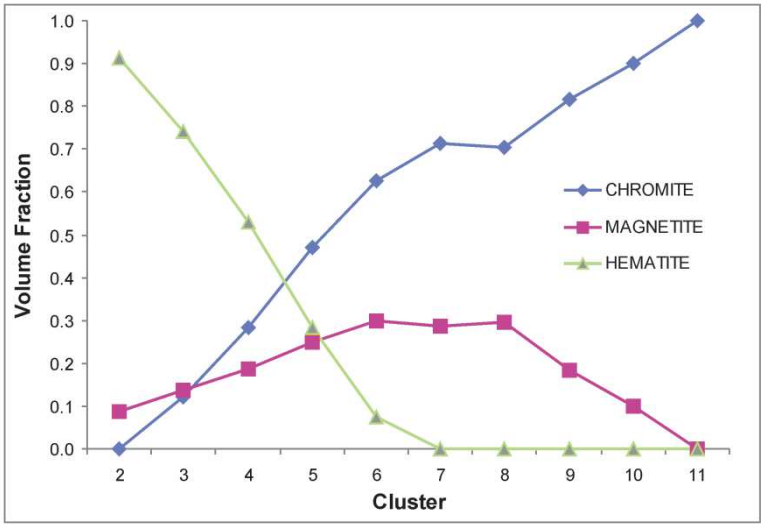

Figure 4. Estimated volume fraction of the three phases identified on the annealed chromite's polished surface for each of the different zones identified according to the twelve-cluster hierarchical cluster analysis.

Observation of the Raman map shows that after 50 days at 700 °C the sample has developed a thin (< 5 µm) layer of pure hematite at the sample surface; the hematite contents gradually decreases and eventually disappears at a depth of about 10 – 30 µm from the surface, while the content of both chromite and magnetite increases – the latter growing up to about 30% volume fraction. Beyond such limit at about 10 – 30 µm from the surface, the magnetite content rapidly drops to zero, so that in the core of the sample only pure chromite is found. It is to notice the presence of trellis-like structures constituted by a mixture of magnetite and chromite. These lines are not uncommon in natural spinels and testify the presence of another phase (usually ilmenite, in Ti-rich spinels) [40,41]. In this case, these intergrowths caused by oxidation of the magnetite/ulvospinel solution create these peculiar features due to the fact that oxygen layers parallel to {111} in the spinel structure and lattice oxygen parallel to {0001} in the ilmenite structure are almost equivalent[42]. These lamellae (usually <1-10 microns) are due to exsolution driven by the oxidation. In the present

case we can invoke the same procedure for the formation of these exsolved lamellae of magnetite within the "pure" chromite area.

4. Discussion

In spinels there are five Raman-active modes, i.e. A_{1g} + E_g + $3F_{2g}$ exhibiting Raman vibrational modes in the 100-800 cm^{-1} spectral region. Strong bands are observed in the region around 400-500 cm^{-1} and 700-800 cm^{-1} assigned to the E_g and A_{1g} modes, respectively [43]. According to D'Ippolito et al. 2015 [43] and references therein, the bands around 600 cm^{-1} are assigned to the third F_{2g} symmetry species, the bands around 480-520 cm^{-1} to the second F_{2g} symmetry species, whereas, the bands around 200-300 cm^{-1} are assigned to the first F_{2g} symmetry species.

In chromite, the peak at the highest Raman shift is commonly attributed to the A_{1g} mode. Synthetic chromite shows a peak at about 674 cm^{-1} [43]. However a shift is often observed and is normally attributed to a non-ideal content of Cr and Fe^{3+}, usually associated to the presence of Al because, in natural spinels, the Al content is usually higher than that of Fe^{3+} (however, in the present case, Al is not present because it was not included in the synthesis, therefore the observed shift should be attributed to a different cause). Reddy and Frost (2005)[44] associated this vibrational mode to the Cr – O stretch; in particular it is assigned to the (Cr^{3+}, Fe^{3+}, Al^{3+})O6 octahedra [31,45]. It must also be noted that some authors associate this mode to O vibrations [32] or to the Fe – O symmetric stretching [33]. In natural Cr-bearing spinelides there is a linear positive correlation between Cr content and the A_{1g} mode [31,45], and the presence of Al is found to influence such correlation. One question is if Fe^{3+} acts in a similar way. Previous structural studies on spinels from the same synthesis revealed that they are stoichiometric with the octahedral site completely filled by two Cr cations [26]. Moreover, the possible presence of Fe^{3+} in both sites could cause the so-called "dragging effect" to the M site distorting the octahedral[46].

The spectral series shows the presence of two peaks at about 380 cm^{-1} and 630 cm^{-1} (shoulder). Peaks in the range 615-630 cm^{-1} have been observed by Kharbish (2018)[47] in natural ferrian chromites with $Fe^{3+}/(Fe^{3+}+Cr+Al)$ ranging from 0.39 to 0.70. For the same samples, Kharbish (2018) found out peaks in the range 333-350 cm^{-1}, far from our 380 cm^{-1} value. However, it can be observed that their intensity follows approximately the same trend as the peak at about 530 cm^{-1}, which is unequivocally associated to the T_{2g} (2) mode in magnetite, this suggesting that these modes might be associated to such phase mixed with different Cr content. It must be noted, however, that peaks at about 380 cm^{-1} and 630 cm^{-1} have also recently been observed by Lenaz and Lughi (2013) in $Mg(Cr,Fe^{3+})_2O_4$ synthetic spinels[34]; in particular, such modes were found to

appear in spinels with more than 70% of Mg-ferrite, when a structure inversion occurs – i.e. Fe^{3+} starts occupying not only the octahedral, but also the tetrahedral site. Menegazzo and Carbonin (1998) and Carbonin et al. (1999)[18,19], in studies about artificially or naturally oxidized Cr-bearing spinelides, suggested the possibility that there are two processes known as maghemitization characterized by the reaction $3Fe^{2+} \rightarrow 2Fe^{3+} + 1\Upsilon$, where Υ is a structural vacancy, and martitization, i.e. the formation of α-Fe_2O_3, hematite. Considering other possible explanations, another cause of structural asymmetries – along with non-perfect stoichiometry and defects – is the presence of residual stresses, e.g. induced by phase transformation. This, rather than generating new modes, might lead to the shift of known ones; one might speculate for example that the mode at 630 cm^{-1} results from a shift of the known A_{1g} mode (which in previous studies has been observed to occur in the 640-670 cm^{-1} range). However, the observation that the positions of almost all peaks (with one exception discussed below) is very similar in the whole spectral series, suggests that residual stresses - if present - are essentially negligible – thus strongly weakening the latter hypothesis. Our hypothesis is that at the beginning of the oxidation process there is the transformation of Fe^{2+} into Fe^{3+} in T site, causing the shift of the A_{1g} mode towards lower values and the presence of the two peaks at 380 and 630 cm^{-1}.

The only peak in the spectral series that shows a marked shift is the T_{2g} mode (at about 530 cm^{-1}), associated to magnetite: this mode is stable in the spectra where magnetite is mixed with hematite (cluster 2 through 6), while it shows a marked shift (from 530 to 545 cm^{-1}), when it is mixed with chromite. One possibility is that these two latter phases possess a common vibrational mode with a slightly different position. Another possible speculation is that the presence of chromite induces a state of stress in the magnetite; although this seems to be unlikely because in that case some stress-induced shift of the peaks of chromite would be expected as well, it cannot be ruled out since the value of the piezospectroscopic coefficients is currently unknown, and could be so low to lead to non-detectable shifts.

Concerning the structural changes of the sample, the results indicate that chromite annealed in air at high temperature undergoes an oxidation process leading to the transformation of chromite to magnetite, and ultimately to hematite. Such oxidation proceeds inwards from the outer surface – which is exposed to the oxidizing atmosphere. The oxidation process also leads to the formation of trellis-like lines, arguably via stress-related mechanisms associated to the phase transformation and consequent volume changes. Further investigations are needed to clarify this matter.

As seen above, the oxidation of chromian spinelides is well known in natural samples. Our study showed that contrarily to the natural samples, alteration began to happen only at a temperature higher than about 600°C. Considering the differences with natural samples it can be said that in the

latter the presence of other cations, such as Mg and Al, other phases, as olivine, and, possibly, fluids lowers the temperature of formation of at least one hundred degrees. In fact, while different authors[21,48] consider a temperature of about 500-600 °C for the formation of the ferritchromite rim, a synthetic chromite annealed at 600 °C shows no evident oxidation while the presence of the ferritchromite rim is evident in crystals annealed at a temperature equal or higher than 700 °C. Consequently, in presence of a limited amount of other cations or other phases, like chromitite pods were spinels show high Cr/(Cr+Al) and Fe^{2+}/(Fe^{2+}+Mg) ratios, the supposed temperature could be different from the real occurred one.

Moreover, it is interesting to notice that this study seems to confirm the ideas suggested by Della Giusta et al. (2011)[49] in their study on possible chromite to magnetite transformation in magnetite ore bodies from Aosta Valley (northwestern Italy) giving new light on possible mechanism of ore deposit formation. Those authors suggested that the Cogne magnetite may represent the last stage of the chromite to magnetite transformation, with the sole survival of the inverse spinel structure. Samples from all the other deposits of Aosta Valley, retaining appreciable amounts of relict Cr-enriched areas, represent a transitional situation, where both normal and inverse structures still coexist. The inhomogeneous chemical composition revealed at the micrometer scale seems to be the consequence of a complex transformation responsible for the survival of microsites the compositions of which recall, but do not fit, those of a chromite proto-ore, with the exceeding chromium removed from the area following the mechanisms suggested by Arai and Akizawa (2014) and Watenpuhl et al. (2014)[50,51].

As for the closed system investigated in the present paper, the considerations that (i) chromium cannot be purged out from the system and (ii) the presence of new chromium-containing phases is not detected during magnetite and hematite formation at the expense of chromite, led to propose that chromium released from the destructed chromite is present as an impurity in the newly formed iron oxides. This hypothesis is confirmed from a comparison with Raman spectra obtained for Cr-doped hematite which shows that, on substitution of Cr at Fe site, all phonon modes are maintained [52]. Moreover, McCarty and Boehme [53] observed an additional band when chromium is substituted for iron in hematite, which shifts almost linearly with increasing Cr content from 664 cm^{-1} (for $Fe_{1.73}Cr_{0.27}O_3$) to 685 cm^{-1} (for $Fe_{0.4}Cr_{1.6}O_3$). In the present work, the same shift is observed moving from cluster 2 (where nearly pure hematite grown in the sample surface is present) to clusters 3-6, related to the inner part of the sample, where the chromium content in hematite is much more higher.

In the field of corrosion science, Ziemniak and Hanson (2002)[24] studied the corrosion behavior of an austenitic stainless steel (UNS S30400) in a 10,000 h test conducted in hydrogenated, ammoniated water at 260 °C. Based on the distribution of the three oxidized alloying constituents (Fe, Cr, Ni) those authors found that the corrosion occurs in a non-selective manner, and that the corrosion film consists of two spinel oxide layers—a ferrite-based outer layer $(Ni_{0.2}Fe_{0.8})(Fe_{0.95}Cr_{0.05})_2O_4$ on top of a chromite-based inner layer $(Ni_{0.2}Fe_{0.8})(Cr_{0.7}Fe_{0.3})_2O_4$. These compositions agree closely with the solvi phases created by immiscibility in the Fe_3O_4–$FeCr_2O_4$ binary. The significance of the above compositions lies in the spinel immiscibility. Although both outer and inner oxide layers are spinels, the ferrite-based outer layer is an inverse spinel while the chromite-based inner layer is a normal spinel. When an alloy undergoes oxidation, one would expect that a single phase oxide (i.e., spinel) would be capable of accommodating the oxidized alloying constituents in a solid solution. However, the existence of two spinel sub-categories imposes certain limitations on the mixing process. The Fe_3O_4–$FeCr_2O_4$ binary, which is relevant to spinel corrosion films on iron-based FeCrNi alloys, is known to exhibit a solution temperature around 880 °C [54]. Below this temperature, complete mixing is not possible and separation into a ferrite-rich spinel and a chromite-rich spinelide occurs. This result is identical within experimental error, to the Fe(III)–Cr(III) distribution observed in the corrosion oxide layers formed on 304 stainless steel.

One additional important implication of our work is to show the potential of Raman spectroscopy and in particular of Raman mapping, combined with the statistical analysis of the large amount of data that can be collected by automated mapping systems. This combination of techniques is now being increasingly appreciated in the fields of materials science and in biomedical and biological applications [55], but has hardly been used for mineralogy studies. We showed that Raman spectra and maps can be easily collected from this kind of samples, non-destructively and without any additional sample preparation with respect to that needed for more standard techniques (XRD, optical and SEM imaging, etc.); actually, no preparation at all is necessary for Raman spectroscopy in itself, as spectra can be collected from virtually any kind of surface.

4. Conclusions

The structural changes occurring in a synthetic chromite $FeCr_2O_4$ sample after annealing treatment were investigated by means of Raman analyses. The results indicate that chromite annealed in air at high temperature undergoes an oxidation process leading to the transformation of chromite to magnetite, and ultimately to hematite. Such oxidation proceeds inwards from the outer surface – which is exposed to the oxidizing atmosphere. The oxidation process also leads to the formation of

trellis-like lines, arguably via stress-related mechanisms associated with the phase transformation and consequent volume changes.

The obtained results confirm the possibility of non-stoichiometry or structural defects causing slight structural asymmetries and the formation of new modes, resulting in a valuable support in characterizing both natural and artificial material.

Moreover, the present study allows us to explore the potential of Raman spectroscopy in the identification and spatial resolution of mineralogical phases, which cannot be identified otherwise by optical or electron microscopy, nor could be spatially resolved by standard X-Ray Diffraction. Raman spectroscopy with mapping capabilities revealed an excellent candidate as a key characterization technique for applications in mineralogy, for its facile applicability and its capability for spatially resolved analysis of the material's structure, composition, and – in prospective – residual stresses [56].

References

[1] M. Younis, M. Saleem, S. Atiq, S. Naseem, Magnetic phase transition and magneto-dielectric analysis of spinel chromites: MCr2O4 (M = Fe, Co and Ni), Ceram. Int. 44 (2018) 10229–10235. https://doi.org/10.1016/j.ceramint.2018.03.024.

[2] D. Lenaz, G.B. Andreozzi, M. Bidyananda, F. Princivalle, Oxidation degree of chromite from Indian ophiolites: A crystal chemical and 57Fe Mössbauer study, Period. Mineral. 83 (2014) 241–255. https://doi.org/10.2451/2014PM0014.

[3] D. Lenaz, H. Skogby, A.M. Logvinova, N.V. Sobolev, F. Princivalle, A micro-Mössbauer study of chromites included in diamond and other mantle-related rocks, Phys. Chem. Miner. 40 (2013) 671–679. https://doi.org/10.1007/s00269-013-0602-8.

[4] I. Pérez, I. Moreno-Ventas, G. Ríos, Chemical degradation of magnesia-chromite refractory used in the conversion step of the pyrometallurgical copper-making process: A thermochemical approach, Ceram. Int. 44 (2018) 18363–18375. https://doi.org/10.1016/j.ceramint.2018.07.052.

[5] L. Xu, M. Chen, N. Wang, S. Gao, Y. Wu, Degradation mechanisms of magnesia-chromite refractory bricks used in oxygen side-blown reducing furnace, Ceram. Int. (2020). https://doi.org/10.1016/j.ceramint.2020.04.020.

[6] V.S. Urusov, Interaction of cations on octahedral and tetrahedral sites in simple spinels, Phys. Chem. Miner. 9 (1983) 1–5. https://doi.org/10.1007/BF00309461.

[7] H.S.C. O'Neill, A. Navrotsky, Cation distributions and thermodynamic properties of binary spinel solid solutions., Am. Mineral. 69 (1984) 733–753.

[8] D. Lenaz, B. Schmitz, Crystal structure refinement of chromites from two achondrites, their T-f(O2) conditions, and implications, Meteorit. Planet. Sci. 52 (2017) 1763–1775. https://doi.org/10.1111/maps.12885.

[9] D. Lenaz, V. Lughi, D. Perugini, M. Petrelli, G. Turco, B. Schmitz, MgAl2O4 spinels from Allende and NWA 763 carbonaceous chondrites: Structural refinement, cooling history, and trace element contents, Meteorit. Planet. Sci. 54 (2019) 3089–3100. https://doi.org/10.1111/maps.13400.

[10] D. Lenaz, B. O'Driscoll, F. Princivalle, Petrogenesis of the anorthosite-chromitite association: crystal-chemical and petrological insights from the Rum Layered Suite, NW Scotland, Contrib. Mineral. Petrol. 162 (2011) 1201–1213. https://doi.org/10.1007/s00410-011-0647-y.

[11] F. Parisi, D. Lenaz, F. Princivalle, L. Sciascia, Ordering kinetics in synthetic Mg (Al, Fe3+) 2O4 spinels: Quantitative elucidation of the whole Al-Mg-Fe partitioning, rate constants, activation energies, Am. Mineral. 99 (2014) 2203–2210.

[12] F. Princivalle, F. Martignago, A. Dal Negro, Kinetics of cation ordering in natural Mg(Al,Cr3+)2 O4 spinels, Am. Mineral. 91 (2006) 313–318. https://doi.org/10.2138/am.2006.1894.
[13] Z. Nédli, F. Princivalle, D. Lenaz, T.M. Tóth, Crystal chemistry of clinopyroxene and spinel from mantle xenoliths hosted in Late Mesozoic lamprophyres (Villány Mts, S Hungary), Neues Jahrb. Mineral. Abh. 185 (2008) 1–10. https://doi.org/10.1127/0077-7757/2008/0107.
[14] B. Lavina, F. Princivalle, A. Della Giusta, Controlled time-temperature oxidation reaction in a synthetic Mg-hercynite, Phys. Chem. Miner. 32 (2005) 83–88. https://doi.org/10.1007/s00269-004-0438-3.
[15] M. Taran, F. Parisi, D. Lenaz, A. Vishnevskyy, Synthetic and natural chromium-bearing spinels: an optical spectroscopy study, Phys. Chem. Miner. 41 (2014) 593–602.
[16] M. Dondi, C. Zanelli, M. Ardit, G. Cruciani, L. Mantovani, M. Tribaudino, G.B. Andreozzi, Ni-free, black ceramic pigments based on Co—Cr—Fe—Mn spinels: A reappraisal of crystal structure, colour and technological behaviour, Ceram. Int. 39 (2013) 9533–9547. https://doi.org/10.1016/j.ceramint.2013.05.072.
[17] G. Menegazzo, S. Carbonin, A.D. Giusta, Cation and vacancy distribution in an artificially oxidized natural spinel, Mineral. Mag. 61 (1997) 411–421. https://doi.org/10.1180/minmag.1997.061.406.07.
[18] G. Menegazzo, S. Carbonin, Oxidation mechanisms in Al–Mg–Fe spinels. A second stage: α–Fe2O3 exsolution, Phys. Chem. Miner. 25 (1998) 541–547. https://doi.org/10.1007/s002690050146.
[19] S. Carbonin, G. Menegazzo, D. Lenaz, F. Princivalle, Crystal chemistry of two detrital Cr-spinels with unusually low values of oxygen positional parameter: Oxidation mechanisms and possible origin, Neues Jahrb. Mineral. Monatshefte. 8 (1999) 359–371.
[20] F. Bosi, G.B. Andreozzi, V. Ferrini, S. Lucchesi, Behavior of cation vacancy in kenotetrahedral Cr-spinels from Albanian eastern belt ophiolites, Am. Mineral. 89 (2004) 1367–1373. https://doi.org/10.2138/am-2004-1003.
[21] D. Lenaz, J. Adetunji, H. Rollinson, Determination of Fe3+/ΣFe ratios in chrome spinels using a combined Mössbauer and single-crystal X-ray approach: Application to chromitites from the mantle section of the Oman ophiolite, Contrib. Mineral. Petrol. 167 (2014) 1–17. https://doi.org/10.1007/s00410-013-0958-2.
[22] H. Rollinson, J. Adetunji, D. Lenaz, K. Szilas, Archaean chromitites show constant Fe3 +/ΣFe in Earth's asthenospheric mantle since 3.8 Ga, Lithos. 282–283 (2017) 316–325. https://doi.org/10.1016/j.lithos.2017.03.020.
[23] M. Velicogna, D. Lenaz, Is 600 °C enough to produce air oxidation in Cr-spinels?, Neues Jahrb. Mineral. Abh. 194 (2017) 125–137. https://doi.org/10.1127/njma/2017/0047.
[24] S.E. Ziemniak, M. Hanson, Corrosion behavior of 304 stainless steel in high temperature, hydrogenated water, Corros. Sci. 44 (2002) 2209–2230. https://doi.org/10.1016/S0010-938X(02)00004-5.
[25] T. Jonsson, B. Pujilaksono, H. Heidari, F. Liu, J.-E. Svensson, M. Halvarsson, L.-G. Johansson, Oxidation of Fe-10Cr in O2 and in O2+H2O environment at 600°C: A microstructural investigation, Corros. Sci. 75 (2013) 326–336. https://doi.org/10.1016/j.corsci.2013.06.016.
[26] D. Lenaz, H. Skogby, F. Princivalle, U. Hålenius, Structural changes and valence states in the MgCr2O4-FeCr2O4 solid solution series, Phys. Chem. Miner. 31 (2004) 633–642. https://doi.org/10.1007/s00269-004-0420-0.
[27] D. Lenaz, H. Skogby, Flux growth of synthetic single crystal spinels in the (Mg, Fe 2+)(Cr, Fe3+)2O4 system, Period. Mineral. 72 (2003) 69–78.
[28] A. Bonifacio, C. Beleites, V. Sergo, Application of R-mode analysis to Raman maps: A different way of looking at vibrational hyperspectral data, Anal. Bioanal. Chem. 407 (2014). https://doi.org/10.1007/s00216-014-8321-7.
[29] H. Ali, R. Ullah, S. Khan, M. Bilal, Raman spectroscopy and hierarchical cluster analysis for the ingredients characterization in different formulations of paracetamol and counterfeit paracetamol, Vib. Spectrosc. 102 (2019) 112–115. https://doi.org/10.1016/j.vibspec.2019.05.002.
[30] O.N. Shebanova, P. Lazor, Raman spectroscopic study of magnetite (FeFe2O4): A new assignment for the vibrational spectrum, J. Solid State Chem. 174 (2003) 424–430. https://doi.org/10.1016/S0022-4596(03)00294-9.

[31] A. Wang, K.E. Kuebler, B.L. Jolliff, L.A. Haskin, Raman spectroscopy of Fe-Ti-Cr-oxides, case study: Martian meteorite EETA79001, Am. Mineral. 89 (2004) 665–680. https://doi.org/10.2138/am-2004-5-601.
[32] I. Chamritski, G. Burns, Infrared- And raman-active phonons of magnetite, maghemite, and hematite: A computer simulation and spectroscopic study, J. Phys. Chem. B. 109 (2005) 4965–4968. https://doi.org/10.1021/jp048748h.
[33] M.A. Legodi, D. de Waal, The preparation of magnetite, goethite, hematite and maghemite of pigment quality from mill scale iron waste, Dyes Pigments. 74 (2007) 161–168. https://doi.org/10.1016/j.dyepig.2006.01.038.
[34] D. Lenaz, V. Lughi, Raman study of MgCr2O4-Fe2+Cr2O4 and MgCr2O4-MgFe23+O4 synthetic series: The effects of Fe2+ and Fe3+ on Raman shifts, Phys. Chem. Miner. 40 (2013) 491–498. https://doi.org/10.1007/s00269-013-0586-4.
[35] M. Testa-Anta, M.A. Ramos-Docampo, M. Comesaña-Hermo, B. Rivas-Murias, V. Salgueiriño, Raman spectroscopy to unravel the magnetic properties of iron oxide nanocrystals for bio-related applications, Nanoscale Adv. 1 (2019) 2086–2103. https://doi.org/10.1039/C9NA00064J.
[36] T. Sundius, Computer fitting of Voigt profiles to Raman lines, J. Raman Spectrosc. 1 (1973) 471–488. https://doi.org/10.1002/jrs.1250010506.
[37] T. S. Alstrøm, M. N. Schmidt, T. Rindzevicius, A. Boisen, J. Larsen, A pseudo-Voigt component model for high-resolution recovery of constituent spectra in Raman spectroscopy, in: 2017 IEEE Int. Conf. Acoust. Speech Signal Process. ICASSP, 2017: pp. 2317–2321. https://doi.org/10.1109/ICASSP.2017.7952570.
[38] L. Hamza, Morphotropic phase boundary in (Na0.5Bi0.5)TiO3-BaTiO3 lead free system: XRD and Raman spectroscopy studies, Ceram. - Silik. 60 (2016) 1–9. https://doi.org/10.13168/cs.2016.0031.
[39] H.G. Schulze, S. Rangan, M.W. Blades, J.M. Piret, R.F.B. Turner, Smoothing Raman Spectra with Contiguous Single-Channel Fitting of Voigt Distributions: An Automated, High-Quality Procedure, Appl. Spectrosc. 73 (2019) 47–58.
[40] H. Helmy, A.-A. Abdel-Karim, W. Elwan, S. El-Shafei, Spinels, Fe-Ti oxide minerals, apatites, and carbonates hosted in the ophiolites of Eastern Desert of Egypt: Mineralogy and chemical aspects, Arab. J. Geosci. 7 (2013). https://doi.org/10.1007/s12517-013-0854-0.
[41] J.-P. Arguin, P. Pagé, S.-J. Barnes, R. Girard, C. Duran, An Integrated Model for Ilmenite, Al-Spinel, and Corundum Exsolutions in Titanomagnetite from Oxide-Rich Layers of the Lac Doré Complex (Québec, Canada), Minerals. 8 (2018) 476. https://doi.org/10.3390/min8110476.
[42] S.E. Haggerty, Opaque mineral oxides in terrestrial igneous rocks, in: Oxide Miner., 2018: pp. 303–502. https://www.scopus.com/inward/record.uri?eid=2-s2.0-85061192423&partnerID=40&md5=019ec02f9acfe6e0a4fa320efb321b8d.
[43] V. D'Ippolito, G.B. Andreozzi, D. Bersani, P.P. Lottici, Raman fingerprint of chromate, aluminate and ferrite spinels, J. Raman Spectrosc. 46 (2015) 1255–1264. https://doi.org/10.1002/jrs.4764.
[44] B.J. Reddy, R.L. Frost, Spectroscopic characterization of chromite from the Moa-Baracoa Ophiolitic Massif, Cuba, Spectrochim. Acta - Part Mol. Biomol. Spectrosc. 61 (2005) 1721–1728. https://doi.org/10.1016/j.saa.2004.07.002.
[45] D. Lenaz, V. Lughi, Raman spectroscopy and the inversion degree of natural Cr-bearing spinels, Am. Mineral. 102 (2017) 327–332. https://doi.org/10.2138/am-2017-5814.
[46] D. Lenaz, H. Skogby, F. Princivalle, U. Hålenius, The MgCr2O4-MgFe2O4 solid solution series: Effects of octahedrally coordinated Fe3+ on T-O bond lengths, Phys. Chem. Miner. 33 (2006) 465–474. https://doi.org/10.1007/s00269-006-0093-y.
[47] S. Kharbish, Raman spectroscopic features of Al- Fe3+- poor magnesiochromite and Fe2+- Fe3+- rich ferrian chromite solid solutions, Mineral. Petrol. 112 (2018) 245–256. https://doi.org/10.1007/s00710-017-0531-1.
[48] E.J. Derbyshire, B. O'Driscoll, D. Lenaz, R. Gertisser, A. Kronz, Compositionally heterogeneous podiform chromitite in the Shetland Ophiolite Complex (Scotland): Implications for chromitite petrogenesis and late-stage alteration in the upper mantle portion of a supra-subduction zone ophiolite, Lithos. 162–163 (2013) 279–300. https://doi.org/10.1016/j.lithos.2012.11.013.

[49] A. Della Giusta, S. Carbonin, U. Russo, Chromite to magnetite transformation: Compositional variations and cation distributions (southern Aosta Valley, Western Alps, Italy), Period. Mineral. 80 (2011) 1–17. https://doi.org/10.2451/2011PM0001.
[50] S. Arai, N. Akizawa, Precipitation and dissolution of chromite by hydrothermal solutions in the Oman ophiolite: New behavior of Cr and chromite, Am. Mineral. 99 (2014) 28–34. https://doi.org/10.2138/am.2014.4473.
[51] A. Watenphul, C. Schmidt, S. Jahn, Cr(III) solubility in aqueous fluids at high pressures and temperatures, Geochim. Cosmochim. Acta. 126 (2014) 212–227. https://doi.org/10.1016/j.gca.2013.10.054.
[52] A. Yogi, D. Varshney, Magnetic and structural properties of pure and Cr-doped haematite: α-Fe2−xCrxO3 (0 ≤ x ≤ 1), J. Adv. Ceram. 2 (2013) 360–369. https://doi.org/10.1007/s40145-013-0084-7.
[53] K.F. McCarty, D.R. Boehme, A Raman study of the systems Fe3−xCrxO4 and Fe2−xCrxO3, J. Solid State Chem. 79 (1989) 19–27. https://doi.org/10.1016/0022-4596(89)90245-4.
[54] V. Cremer, Die mischkristallbildung im systemchromit-magnetit-hercynit zwischen 1000° and 500°C., Neues Jahrb. Für Mineral. - Abh. (1969) 184–205.
[55] A. Bonifacio, C. Beleites, F. Vittur, E. Marsich, S. Semeraro, S. Paoletti, V. Sergo, Chemical imaging of articular cartilage sections with Raman mapping, employing uni- and multi-variate methods for data analysis, Analyst. 135 (2010) 3193–3204. https://doi.org/10.1039/c0an00459f.
[56] L. Ciacchi, G. Grégori, V. Lughi, A. Rossi, V. Sergo, Piezo-Spectroscopy: a Materials Science Perspective, 1999.

Declaration of interests

The authors declare that they have no known competing financial interests or personal relationships that could have appeared to influence the work reported in this paper.